ARTHRITIS & RHEUMATOLOGY
Vol. 68, No. 1, January 2016, pp 210–217
DOI 10.1002/art.39421

Endothelial Cells Expressing Endothelial and Mesenchymal Cell Gene Products in Lung Tissue From Patients With Systemic Sclerosis–Associated Interstitial Lung Disease

Fabian A. Mendoza,[1] Sonsoles Piera-Velazquez,[1] John L. Farber,[1] Carol Feghali-Bostwick,[2] and Sergio A. Jiménez[1]

Objective. **To examine whether lung endothelial cells (ECs) from patients with systemic sclerosis (SSc)–associated interstitial lung disease (ILD) express mesenchymal cell–specific proteins and gene transcripts, indicative of the occurrence of endothelial-to-mesenchymal phenotypic transition (EndoMT).**

Methods. **Lung tissue from 6 patients with SSc-associated pulmonary fibrosis was examined by histopathology and immunohistochemistry. Confocal laser microscopy was utilized to assess the simultaneous expression of EC and myofibroblast molecular markers. CD31+CD102+ ECs were isolated from the lung tissue of 2 patients with SSc-associated ILD and 2 normal control subjects, and the expression of EC and mesenchymal cell markers and other relevant genes was analyzed by quantitative polymerase chain reaction, immunofluorescence microscopy, and Western blotting.**

Results. **Immunohistochemical staining revealed cells expressing the EC-specific marker CD31 in the subendothelial, perivascular, and parenchymal regions of the lungs from all SSc patients. Confocal microscopy identified cells displaying simultaneous expression of von Willebrand factor and α-smooth muscle actin in small and medium-sized arterioles in the SSc lung tissue but not in normal control lungs. CD31+CD102+ ECs isolated from SSc lungs expressed high levels of mesenchymal cell–specific genes (type I collagen, type III collagen, and fibronectin), EC-specific genes (type IV collagen and VE-cadherin), profibrotic genes (transforming growth factor β1 and connective tissue growth factor), and genes encoding EndoMT-related transcription factors (TWIST1 and SNAI2).**

Conclusion. **Cells coexpressing EC- and mesenchymal cell–specific molecules are present in the lungs of patients with SSc-associated ILD. CD31+CD102+ ECs isolated from SSc lungs simultaneously expressed mesenchymal cell– and EC-specific transcripts and proteins. Collectively, these observations demonstrate the occurrence of EndoMT in the lungs of patients with SSc-associated ILD.**

Systemic sclerosis (SSc) is a systemic autoimmune disease of unknown etiology that is characterized by progressive fibrosis of the skin and multiple internal organs, as well as severe fibroproliferative vasculopathy affecting the microvasculature, resulting in severe vessel narrowing or even complete vascular obliteration (1–3). The pathogenetic mechanisms responsible for the fibrotic process and the severe vascular alterations in SSc are complex and have not been fully elucidated (4–6). Numerous recent studies have demonstrated that activated myofibroblasts are the cells ultimately responsible for the exaggerated deposition of extracellular matrix (ECM) macromolecules in the skin, the parenchyma of affected organs such as the lungs and the heart, and the subendothelial space of small and

The contents of this article are solely the responsibility of the authors and do not necessarily represent the official views of the National Institutes of Health.

Supported by the NIH (National Institute of Arthritis and Musculoskeletal and Skin Diseases Core Center grant P30-AR-061271 to Dr. Feghali-Bostwick, grant K24-AR-060297 to Dr. Feghali-Bostwick, and grant R01-AR-19616 [Biochemical and Vascular Alterations in Scleroderma] to Dr. Jiménez).

[1]Fabian A. Mendoza, MD, Sonsoles Piera-Velazquez, PhD, John L. Farber, MD, Sergio A. Jiménez, MD: Thomas Jefferson University, Philadelphia, Pennsylvania; [2]Carol Feghali-Bostwick, PhD: Medical University of South Carolina, Charleston.

Drs. Mendoza and Piera-Velazquez contributed equally to this work.

Address correspondence to Sergio A. Jiménez, MD, Jefferson Institute of Molecular Medicine, Thomas Jefferson University, 233 South 10th Street, Room 509 BLSB, Philadelphia, PA 19107-5541. E-mail: sergio.jimenez@jefferson.edu.

Submitted for publication April 20, 2015; accepted in revised form September 1, 2015.

Table 1. Selected clinical and demographic characteristics of the patients with systemic sclerosis (SSc)–associated interstitial lung disease*

	Patient 1	Patient 2	Patient 3	Patient 4	Patient 5	Patient 6
SSc subtype	Diffuse	Limited	Unspecified	Unspecified	Unspecified	Unspecified
Type of lung tissue sample	Biopsy	Biopsy	Transplant	Transplant	Transplant	Transplant
Age at time of sampling, years	53	45	68	30	52	64
Sex	Male	Female	Female	Female	Female	Male
Time from onset of skin disease, years	2	5	Unspecified	7	10	15
Time from onset of respiratory symptoms, months	6	8	Unspecified	Unspecified	Unspecified	Unspecified
Smoker	No	No	No	No	No	Yes
Progressive respiratory symptoms	Yes	Yes	Yes	Yes	Yes	Yes
Pulmonary hypertension	No	No†	No	No	No	No
ANA titer or status	1/640	1/640	Positive	Positive	Positive	Positive
Anti–Scl-70/ACAs	Negative	ACAs	NA	NA	NA	NA

* ANA = antinuclear antibody; ACAs = anticentromere antibodies; NA = not available.
† Patient developed pulmonary hypertension 10 months after the lung biopsy was performed.

medium-sized arteries in SSc (7–9). Activated myofibroblasts are a unique class of mesenchymal cells characterized by specific biologic functions, including a motile phenotype, expression of α-smooth muscle actin (α-SMA), increased production of fibrillar type I collagen (COL1) and type III collagen (COL3), and reduction in the expression of genes encoding ECM-degradative enzymes (10,11).

Activated myofibroblasts in fibrotic tissue can emerge from several sources (11–13), including through the expansion of resident tissue fibroblasts (14), via the migration and tissue accumulation of bone marrow–derived circulating fibrocytes (15,16), or by transition of epithelial cells, pericytes, and Gli-1–positive perivascular progenitor cells to a mesenchymal phenotype (17–19). More recently, it has been demonstrated that endothelial cells (ECs) are also capable of undergoing a phenotypic change into mesenchymal cells, in a process known as endothelial-to-mesenchymal transition (EndoMT) (20–23). Although EndoMT was initially considered to occur only during cardiovascular embryonic development (24), accumulating evidence indicates that this process occurs in various experimentally induced models of tissue fibrosis (20–23,25–28), and may play a role in the pathogenesis of certain human fibrotic and vascular disorders, including idiopathic and SSc-associated pulmonary arterial hypertension (29–33).

In the present study, we provide immunohistologic and confocal microscopy evidence demonstrating that cells displaying specific EC molecular markers are present in the subendothelial, perivascular, and parenchymal regions of the lungs of patients with SSc-associated interstitial lung disease (ILD), and that ECs expressing myofibroblast-specific molecular markers can be identified in the endothelium and subendothelial space of small and medium-sized arteries in the lungs of patients with SSc. We further show that highly purified CD31+CD102+ ECs isolated from SSc-affected lungs produce numerous mesenchymal cell–specific proteins and display the simultaneous expression of mesenchymal cell– and EC-specific transcripts as well as the expression of EndoMT-associated transcription factors. These observations provide strong support to the hypothesis that a population of activated myofibroblasts responsible for the progressive intimal fibrosis, vascular occlusion, and pulmonary fibrosis in SSc-associated ILD originate from lung ECs through the EndoMT process. This novel mechanism may represent an important and novel therapeutic target for the severe, and currently fatal, complications of SSc-associated fibroproliferative vasculopathy and pulmonary fibrosis.

PATIENTS AND METHODS

Tissue samples. Lung tissue samples from 6 patients with SSc-associated ILD were studied. Two of the lung samples were obtained by surgical open lung biopsy performed at Thomas Jefferson University Hospital (patients 1 and 2 in Table 1), and the other 4 lung samples were from patients who had undergone lung transplantation at the University of Pittsburgh Medical Center. The surgical biopsies and the lung transplantations were performed following the patients' provision of informed consent and according to Institutional Review Board–approved protocols from Thomas Jefferson University and the University of Pittsburgh Medical Center. Two normal lung samples obtained from subjects at the time of necropsy served as normal controls for all procedures. Both of the donors of the normal lung tissue died of cerebrovascular accidents. One of the normal control samples was obtained from a 55-year-old female subject at the University of Pittsburgh Medical Center, and the other normal control sample was obtained from a 62-year-old female subject at the National Disease Research Interchange (Philadelphia, PA). These 2 subjects did not have a clinical history of pulmonary disease, and find-

ings on chest radiographs obtained from both subjects before their demise were normal.

Histopathology, immunohistochemistry, and confocal laser microscopy. Slides containing paraffin-embedded lung tissue sections were examined histopathologically by staining with hematoxylin and eosin and Masson's trichrome, and also by immunohistochemical staining with specific EC and mesenchymal (myofibroblast) cell markers. The SSc and normal lung tissue samples were also examined by confocal laser microcopy, as described previously (34). In all immunohistochemical and confocal laser microscopy studies, samples incubated without primary antibody were used as negative controls.

For immunohistochemistry, the following primary antibodies were used: anti-CD31 (Neomarkers), anti–von Willebrand factor (anti-vWF; Dako), anti-COL1 (Santa Cruz Biotechnology), anti-COL3 (Fitzgerald), and anti–α-SMA (Abcam). For single antibody labeling, paraffin-embedded lung tissue sections were immunoassayed with the peroxidase method, using the indicated antibodies. For confocal laser microscopy, paraffin-embedded samples were deparaffinized and dehydrated following antigen retrieval with a citric acid buffer, as described previously (34). Slides were first incubated with blocking IgG solution for 1 hour, and then incubated overnight with one of the following antibodies: anti-CD31 (1:50 dilution), anti–α-SMA (1:200 dilution), anti-vWF (1:50 dilution), anti-COL1 (1:200 dilution), or anti-COL3 (1:200 dilution). IgG binding was revealed following incubation with an F(ab′) sheep anti-rabbit Cy3 antibody and an F(ab′) sheep anti-mouse fluorescein isothiocyanate–conjugated antibody (Sigma) for 1 hour. Nuclei were counterstained with DAPI (Jackson ImmunoResearch). Samples were examined with a Zeiss 51 confocal laser microscope, to evaluate the colocalization of immunoreactivity with polyclonal and monoclonal antibodies in paired combinations of either anti-CD31 or anti-vWF with either anti–α-SMA, anti-COL1, or anti-COL3.

Isolation of human lung ECs. CD31+CD102+ ECs were isolated from the lungs of 2 patients with SSc-associated pulmonary fibrosis (patients 3 and 4 in Table 1) and the 2 normal control lungs, using a modification of previously described methods (35,36). Briefly, lung tissue samples were minced with a scalpel and enzymatically digested with clostridial collagenase (30 mg/100 ml in 0.1% bovine serum albumin [BSA]; Worthington) at 37°C for 1 hour, to obtain a single-cell suspension. Following removal of contaminating erythrocytes and inflammatory cells, the isolated cell suspension was used for isolation of ECs and immunomagnetic selection with rabbit anti-human CD31 antibodies, followed by magnetic bead separation using goat anti-rabbit IgG-conjugated microbeads (1:5; Miltenyi Biotec). The isolated CD31+ ECs were cultured in EC culture medium (ScienCell Research Laboratories) containing 5% fetal bovine serum, 100 units/ml penicillin, and 100 μg/ml streptomycin in 2% gelatin–precoated tissue culture dishes for 5–10 days.

Following expansion, the cells were resuspended and further purified using a second immunologic separation with rabbit anti-human CD102 antibodies, to obtain a highly purified preparation of CD31+CD102+ ECs. The purified CD31+CD102+ ECs were plated on 2% gelatin–coated plastic dishes. Thereafter, cell morphology was assessed by phase contrast microscopy, and the phenotype of the ECs was confirmed by evaluating the cellular uptake of DiI-acetylated low-density lipoprotein (Biomedical Technologies), as previously described (36).

To further evaluate the EC-specific functional activity of the CD31+CD102+ cells isolated from the lungs of patients with SSc, the cells were cultured on plates coated with Matrigel (BD Biosciences) at 37°C in an atmosphere of 5% CO_2, and microtube formation was examined during a 12-day culture period. All studies were performed with cells in early passage (lower than passage 5) to assure the preservation of their original phenotype.

Immunofluorescence staining. For indirect immunofluorescence analysis, CD31+CD102+ lung ECs were seeded onto glass culture slides, and then fixed with 3.7% formaldehyde and permeabilized with 0.1% Triton X-100 in phosphate buffered saline (PBS) for 3 minutes. Slides were washed with PBS and blocked with PBS containing 1% BSA at room temperature for 1 hour, and then incubated with primary antibodies against α-SMA (1:200 dilution), CD31 (1:50 dilution), and vWF (1:50 dilution). In other studies, EC monolayers were examined by immunofluorescence with antibodies to the EC-specific marker VE-cadherin (1:100 dilution; Cell Signaling Technology). Slides were then incubated with Cy3-conjugated secondary antibodies (1:500), followed by counterstaining of nuclei with DAPI.

Western blot analysis. Aliquots of culture medium containing proteins secreted by CD31+CD102+ lung ECs were processed for Western blotting under denaturing conditions. Equal-volume aliquots of culture medium were resolved by sodium dodecyl sulfate–polyacrylamide gel electrophoresis, and transferred to nitrocellulose membranes (Invitrogen). The blots were blocked for 1 hour in Odyssey blocking buffer (Li-Cor). The membranes were incubated overnight at 4°C with either a polyclonal anti-COL1 antibody (Southern Biotech) or a polyclonal anti-COL3 antibody (Sigma-Aldrich) in the same blocking buffer. Thereafter, the membranes were washed with PBS–0.2% Tween 20 and incubated for 1 hour with the appropriate horseradish peroxidase–conjugated secondary antibodies (GE Healthcare), diluted 10,000-fold in Odyssey blocking buffer. Signals were detected and quantitated using an Odyssey Imagen System (Li-Cor). For quantitative analysis of the Western blots, the intensity of fluorescence of the protein bands was corrected for the amount of DNA (in μg) in the corresponding tissue culture plates, representing the number of cells that were used to obtain the samples.

Quantitative reverse transcription–polymerase chain reaction (PCR). CD31+CD102+ lung EC preparations from the lung tissue of 2 normal subjects and 2 patients with SSc-associated ILD were cultured in duplicate wells of 12-well gelatin-treated plastic tissue culture dishes for 72 hours, and then harvested with a cell lifter, washed in cold PBS, and processed for RNA extraction (RNeasy kit; Qiagen), including a genomic DNA digestion step. Total RNA (1 μg) was reverse-transcribed using Superscript II reverse transcriptase (Invitrogen), to generate first-strand complementary DNA. EC transcript levels were quantified using SYBR Green real-time PCR, as described previously (37). The primers used in the PCR analyses are available upon request from the corresponding author. The number of messenger RNA copies in each PCR was corrected for the 18S endogenous control transcript levels. The specificity of the primers was established at the end of the PCR amplification, with the use of melting curve analysis.

Statistical analysis. Comparative threshold cycle analysis of gene expression was performed using DataAssist software (version 3.0; Applied Biosystems), as described previously

(37). The data obtained from SSc lung ECs from each of 2 patients were compared to the mean values obtained in EC preparations from the 2 normal control lungs, and results are expressed as the fold change in gene expression.

RESULTS

Clinical and demographic characteristics of the patients with SSc-associated ILD. The clinical features of the SSc patients whose lung tissues were studied are shown in Table 1. None of the patients had clinical features of pulmonary arterial hypertension at the time that the tissue samples were obtained. All patients were tested for the presence of pulmonary arterial hypertension with the use of transthoracic echocardiograms, and the 4 patients who underwent lung transplantation also underwent right-sided heart catheterizations. None of the echocardiograms and right-sided heart catheterization studies showed any evidence of pulmonary arterial hypertension at the time that the lung biopsy samples were obtained.

Findings of histopathologic and immunohistologic analyses. All 6 lung tissue samples from the patients with SSc-associated ILD displayed varying degrees of interstitial fibrosis, along with a pattern of infiltration of inflammatory mononuclear cells. Numerous small and medium-sized arteries in all samples showed marked intimal proliferation, resulting in narrowing of the vessel lumen and, sometimes, complete obliteration of the affected vessel, as illustrated in Figure 1A.

The EC marker CD31 was used in immunohistologic analyses to identify ECs present in the lung tissue. As expected, CD31-positive cells were detected at sites lining the vessel lumens, as illustrated in Figures 1B–F. However, CD31-positive cells were also observed beneath the endothelial layer embedded within the subendothelial space, a site that contained numerous elongated mesenchymal cells (Figures 1B and C), as well as in the perivascular tissue and within the lung parenchyma, as illustrated in Figures 1D–F. These alterations were present in all lung tissue samples from patients with SSc-associated ILD, as illustrated in SSc patient 2 (Figures 1B–D), patient 3 (Figure 1E), and patient 5 (Figure 1F). However, they were not present in the normal lung tissue samples (results not shown).

Findings of confocal laser microscopy. Confocal laser microscopy showed colocalization of vWF and α-SMA in the endothelium and within the subendothelial compartment in all SSc-associated ILD lung tissue samples (Figures 2A–C). In contrast, samples from normal controls did not show any cells coexpressing the EC and mesenchymal cell markers (results not shown). The

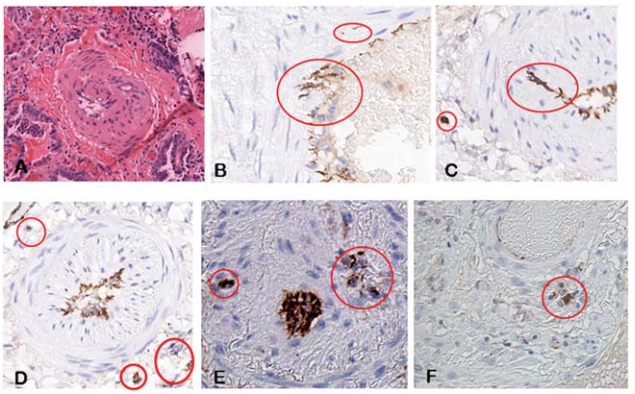

Figure 1. Histopathologic and immunohistologic assessments of lung tissue from patients with systemic sclerosis (SSc)–associated interstitial lung disease (ILD). **A,** Hematoxylin and eosin staining of a small artery in the lung of a patient with SSc-associated ILD. Note the severe narrowing of the vessel lumen as a result of the accumulation of elongated mesenchymal cells and large amounts of fibrous tissue in the subendothelial intimal space. **B** and **C,** Immunohistochemical staining of lung tissue for the endothelial cell (EC)–specific marker CD31. In the lung tissue from the same patient as in **A**, the presence of CD31-positive cells is evident in the subendothelial space next to their expected endothelial location (**B**), while in the lung tissue from another patient, 2 ECs bearing the CD31 marker are embedded within the neointimal tissue removed from the endothelium, and a CD31-positive cell cluster is detected within the fibrotic lung parenchyma (**C**). **D–F,** Immunohistologic staining of the lung tissue from 3 additional patients, showing similar distributions of CD31-positive cells. Circles denote the cells staining positive. Original magnification $\times$ 200. Color figure can be viewed in the online issue, which is available at http://onlinelibrary.wiley.com/journal/doi/10.1002/art.39421/abstract.

colocalization of vWF and α-SMA was observed in both small and medium-sized arterioles. However, it was quite heterogeneous, with some vessels displaying numerous ECs coexpressing both markers, as illustrated in Figures 2A–C, whereas in other vessels, only a few ECs exhibited coexpression or lack of expression was found. Owing to this heterogeneity, it was not possible to obtain an accurate quantitative assessment of the frequency of cells coexpressing both EC and mesenchymal cell markers in the SSc lung tissue.

In addition, we observed that, in contrast to the findings in normal control lungs (as illustrated in Figure 2D), in SSc lungs the EC layer of numerous vessels displayed areas of detachment from the vessel wall and, in some of the vessels, variable portions of vessel lumen appeared completely denuded from the endothelial lining, as illustrated in Figure 2E. Moreover, most ECs in the SSc lung tissue samples displayed very weak or undetectable staining for CD31 (Figures 2E and F), as compared to the very intense staining for CD31 in the vessels of the normal control lungs (Figure 2D). Marked subendothelial accumulation of COL1 (results not

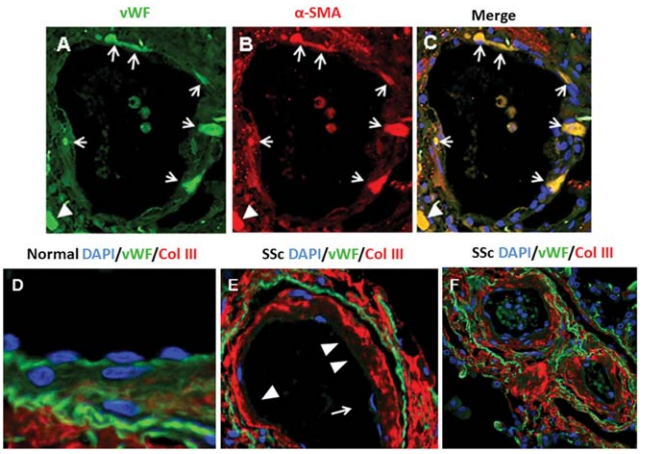

Figure 2. Confocal microscopy staining for von Willebrand factor (vWF; green) and α-smooth muscle actin (α-SMA; red) in a small arteriole in the lung of a patient with systemic sclerosis (SSc)–associated interstitial lung disease (ILD) (**A–C**) and for the type III collagen gene (COL3; red) and CD31 (green) in medium-sized arterioles in a normal control lung (**D**) or lung tissue from patients with SSc-associated ILD (**E** and **F**). Essentially all of the vWF-stained cells present within the endothelium and subendothelial tissue also expressed the mesenchymal cell marker α-SMA (**C**) (yellow). In the normal control vessels (**D**), intense endothelial staining for CD31 is evident, the endothelium appears continuous and well attached to the vessel wall structures, and COL3 staining is only present beyond the elastic lamina. In vessels from a patient with SSc-associated ILD (**E**), the endothelial lining is detached from the vessel wall (**arrow**), some areas of denuded endothelium are noticeable (**arrowheads**), and staining for CD31 is noticeably weaker in the endothelial layer as compared to that in the normal control vessels. In the vessels from another patient with SSc-associated ILD (**F**), intense and abundant staining for COL3 is evident in the subendothelial, medial, and adventitial layers. DAPI was used for counterstaining of nuclei. Original magnification × 400.

shown) and COL3 (Figures 2E and F) was also observed, with various degrees of severity, in all small and medium-sized arterioles throughout the SSc lung tissue samples.

Findings of indirect immunofluorescence analysis of CD31+CD102+ lung ECs and analyses of in vitro microtube formation. To confirm the purity of the ECs isolated from the SSc lungs, dark field microscopy, indirect immunofluorescence, and microtube formation analysis of the cultured CD31+CD102+ ECs from SSc lungs were performed. Dark field microscopy showed the typical cobblestone morphology of ECs in monolayer cultures, and immunofluorescence demonstrated intense staining for the EC-specific marker VE-cadherin (Figure 3A) essentially in all cells, confirming the high level of EC purity in the samples studied. Furthermore, culture of the cells on a Matrigel substrate resulted in the formation of numerous microtubes (Figure 3B), indicative of the preservation of EC functional activities by the purified cells.

Findings of gene expression and Western blot analyses of CD31+CD102+ lung ECs. Gene expression in immunopurified CD31+CD102+ ECs obtained from the lung tissue of 2 patients with SSc-associated ILD was assessed relative to the mean gene expression in immunopurified CD31+CD102+ ECs from 2 normal control lungs (Figure 4A). The results demonstrated a very strong expression of COL1A1 and COL3A1 in the CD31+CD102+ purified ECs from the lungs of the 2 SSc patients, with gene expression values that were up to 21 times and 26 times higher than those in CD31+CD102+ ECs purified from the normal control lungs. The expression of the fibronectin 1 (FN1) and α-SMA (ACTA2) genes and other profibrotic genes, such as those for transforming growth factor β1 (TGFβ1) and connective tissue growth factor (CTGF), as well as the expression of several EndoMT-related genes, such as SNAI2 and TWIST1, was also substantially increased in the CD31+CD102+ ECs from the lungs of SSc patients (Figure 4A).

Western blots of the culture medium from CD31+CD102+ ECs isolated from the lungs of 2 patients with SSc-associated ILD confirmed the gene expression results. Statistically significantly higher amounts of type I collagen and type III collagen proteins were found in CD31+CD102+ ECs from the culture medium of SSc lung tissue compared to that from the culture medium of the 2 normal control lungs (Figure 4B).

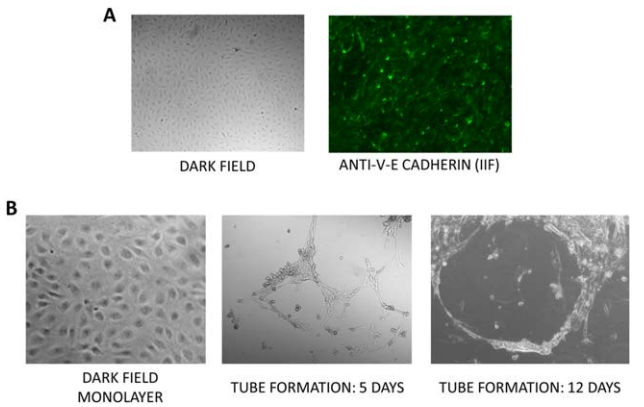

Figure 3. Morphologic and indirect immunofluorescence (IIF) analyses and assessment of in vitro microtube formation in cultured CD31+CD102+ endothelial cells (ECs) isolated from the lung tissue of patients with systemic sclerosis–associated interstitial lung disease. **A,** Dark contrast microscopic image of ECs (left) and results of immunofluorescence analysis of ECs for VE-cadherin (right). **B,** Dark contrast microscopic image of monolayer cultures of ECs (gelatin-coated) (left), and microtube formation in ECs after 5 days and 12 days in Matrigel culture (middle and right). Original magnification × 400 in **A**; × 200 in **B**.

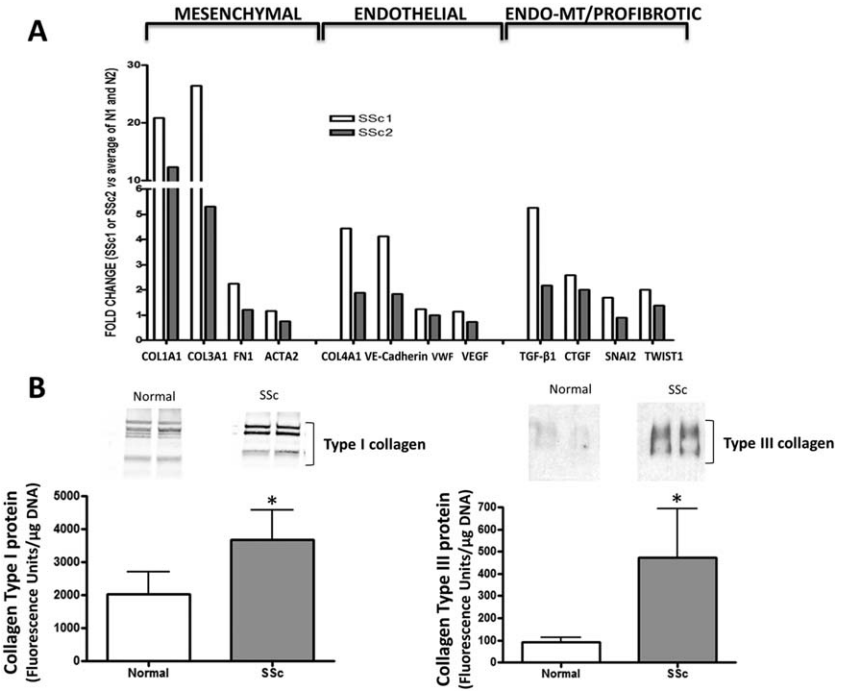

Figure 4. Quantitative polymerase chain reaction (PCR) assessment and Western blot analysis of expression levels of selected genes and proteins in CD31+CD102+ endothelial cells (ECs) from the lung tissue of patients with systemic sclerosis (SSc)–associated interstitial lung disease. **A,** Quantitative PCR of 2 different preparations of CD31+CD102+ ECs from the lungs of 2 SSc patients (SSc 1 and SSc 2) and 2 normal controls (N1 and N2). Shown are transcript measurements, analyzed in duplicate, for interstitial collagen genes (type I collagen A1 [COL1A1] and type III collagen A1 [COL3A1]), fibronectin 1 (FN1), α-smooth muscle actin (ACTA2), EC-specific genes (type IV collagen A1 [COL4A1], VE-cadherin, von Willebrand factor [vWF], and vascular endothelial growth factor [VEGF]), profibrotic genes (transforming growth factor β1 [TGFβ1] and connective tissue growth factor [CTGF]), and endothelial-to-mesenchymal phenotypic transition (EndoMT)–related transcription factors (SNAI2 and TWIST1). Expression levels are shown as the fold change in the lung tissue from each SSc patient compared to the mean levels in the 2 normal controls. **B,** Top, Representative Western blots showing secretion of type I and type III collagens in culture medium of CD31+CD102+ ECs from the lungs of 2 SSc patients and 2 normal controls. Bottom, Quantitative analysis of the results of Western blotting. Bars show the mean ± SEM fluorescence units (corrected for DNA content) in duplicate cultures from each cell line in 3 separate experiments. $* = P < 0.05$ versus normal control lungs.

DISCUSSION

The generation of activated myofibroblasts, which are distinguished from quiescent resident fibroblasts by the initiation of expression of α-SMA and the increased production of fibrillar type I and type III collagens (9–11), is a crucial mechanism in the development of tissue fibrosis in SSc (7–9). Recently, EndoMT has been recognized as an important mechanism in the generation of activated myofibroblasts, a cell type found to be involved in the development of tissue fibrosis in several experimentally induced animal models (20–23,25–28) as well as in some human fibrotic diseases (29–33). Despite its potential role in the pathogenesis of numerous human disorders, the detailed mechanisms involved in EndoMT have not been fully elucidated, although the crucial role of TGFβ in its initiation and maintenance, as well as the participation of several transcription factors involved in cellular transdifferentiation, including SNAI1, SNAI2/SLUG, and TWIST1, has been well documented (20–23,38,39).

Herein, we provide immunohistopathologic evidence of the presence of cells expressing EC-specific molecular markers in the subendothelial neointima as well as in the perivascular regions and in the parenchyma of lung tissue from patients with SSc-associated ILD. Furthermore, we describe confocal microscopy studies demonstrating the presence of numerous cells simultaneously expressing EC and mesenchymal cell molecular markers in small and medium-sized arterioles within the SSc lungs. Similar findings were recently described in the pulmonary arteries of patients with primary pulmonary arterial hypertension (32), as well as in the arterioles of patients with SSc-associated pulmonary hypertension (33), but were not present in pulmonary vessels from healthy controls (32,33).

The frequency of cells coexpressing EC and myofibroblast markers was assessed in the lung microvasculature of patients with SSc-associated pulmonary hypertension, and was found to occur in fewer than 5% of ECs in the pulmonary arterioles (33). In our study, we found that the frequency of cells simultaneously expressing EC- and mesenchymal cell–specific markers was substantially higher, although their occurrence was quite heterogeneous, with some vessels showing that essentially all ECs coexpressed vWF and α-SMA (as illustrated in Figures 2A–C), whereas other vessels contained only a few ECs displaying coexpression, and still other vessels did not show any ECs coexpressing vWF and α-SMA staining. However, owing to the heterogeneity of coexpression on the vessels examined, the low intensity of staining for EC-specific markers in most SSc cells, and the frequent occurrence in SSc lung tissue of abundant and quite variable numbers of inflammatory cells in the subendothelial and perivascular regions, it was not possible to provide an accurate quantitation of the frequency of cells displaying EndoMT in SSc-associated ILD.

An important observation in the present study is that immunopurified CD31+CD102+ lung ECs isolated and expanded in vitro from the lung tissue of patients with SSc-associated ILD exhibited marked upregulation in the expression and production of interstitial type I and type III collagens, and increased levels of transcripts for the potent profibrotic growth factors TGFβ1 and CTGF. These cells also expressed high levels of transcripts for several other EndoMT-related proteins, such as the transcription factors TWIST1 and SNAI2. The marked increase in the expression of TWIST1 in CD31+CD102+ ECs isolated from SSc lungs observed in our study is similar to that found in explanted lung ECs from patients with idiopathic pulmonary arterial hypertension, a finding that was considered to indicate the occurrence of TWIST1-driven EndoMT in vivo (32).

Collectively, the novel observations described in our study provide strong evidence of the occurrence of EndoMT in small and medium-sized arterioles in the lungs of patients with SSc-associated ILD, and suggest that EndoMT may play a role in the development of the severe fibroproliferative vasculopathy and progressive parenchymal fibrosis that are the hallmarks of the pulmonary involvement in SSc (40–42). These results also suggest that greater understanding of the molecular mechanisms involved in EndoMT and its pharmacologic modulation may represent a novel therapeutic approach for the management of fibroproliferative vasculopathy in patients with SSc-associated tissue fibrosis.

ACKNOWLEDGMENTS

We thank Alma Makul and Kerri Fasino for their expert technical assistance and Kenneth Brown, Matthew Landmesser, and Ruth Johnson for their assistance in the preparation of the manuscript.

AUTHOR CONTRIBUTIONS

All authors were involved in drafting the article or revising it critically for important intellectual content, and all authors approved the final version to be published. Dr. Jiménez had full access to all of the data in the study and takes responsibility for the integrity of the data and the accuracy of the data analysis.

Study conception and design. Mendoza, Piera-Velazquez, Jiménez.
Acquisition of data. Mendoza, Piera-Velazquez, Farber, Feghali-Bostwick.
Analysis and interpretation of data. Mendoza, Piera-Velazquez, Feghali-Bostwick, Jiménez.

REFERENCES

1. Varga J, Abraham D. Systemic sclerosis: a prototypic multisystem fibrotic disorder. J Clin Invest 2007;117:557–67.
2. Gabrielli A, Avvedimento EV, Krieg T. Scleroderma. N Engl J Med 2009;360:1989–2003.
3. Matucci-Cerinic M, Kahaleh B, Wigley FM. Systemic sclerosis (scleroderma, SSc) is a vascular disease. Arthritis Rheum 2013; 65:1953–62.
4. Jimenez SA, Derk CT. Following the molecular pathways toward an understanding of the pathogenesis of systemic sclerosis. Ann Intern Med 2004;140:37–50.
5. Katsumoto TR, Whitfield ML, Connolly MK. The pathogenesis of systemic sclerosis. Annu Rev Pathol 2011;6:509–37.
6. Pattanaik D, Brown M, Postlethwaite BC, Postlethwaite AE. Pathogenesis of systemic sclerosis. Front Immunol 2015;6:272.
7. Beon M, Harley RA, Wessels A, Silver RM, Ludwicka-Bradley A. Myofibroblast induction and microvascular alteration in scleroderma lung fibrosis. Clin Exp Rheumatol 2004;22:733–42.
8. Gilbane AJ, Denton CP, Holmes AM. Scleroderma pathogenesis: a pivotal role for fibroblasts as effector cells. Arthritis Res Ther 2013;15:215.
9. Kendall RT, Feghali-Bostwick CA. Fibroblasts in fibrosis: novel roles and mediators. Front Pharmacol 2014;5:123.
10. Hinz B, Phan SH, Thannickal VJ, Prunotto M, Desmouliere A, Varga J, et al. Recent developments in myofibroblast biology: paradigms for connective tissue remodeling. Am J Pathol 2012; 180:1340–55.
11. Hinz B, Phan SH, Thannickal VJ, Galli A, Bochaton-Piallat ML, Gabbiani G. The myofibroblast: one function, multiple origins. Am J Pathol 2007;170:1807–16.
12. McAnulty RJ. Fibroblasts and myofibroblasts: their source, function and role in disease. Int J Biochem Cell Biol 2007;39:666–71.
13. Falke LL, Gholizadeh S, Goldschmeding R, Kok RJ, Nguyen TQ. Diverse origins of the myofibroblast—implications for kidney fibrosis. Nat Rev Nephrol 2015;11:233–44.
14. Poslethwaite AE, Shigemitsu H, Kanagat S. Cellular origins of fibroblasts: possible implications for organ fibrosis in systemic sclerosis. Curr Opin Rheumatol 2004;16:733–8.
15. Strieter RM, Keeley EC, Hughes MA, Burdick MD, Mehrad B. The role of circulating mesenchymal progenitor cells (fibrocytes) in the pathogenesis of pulmonary fibrosis. J Leukoc Biol 2009; 86:1111–8.
16. Herzog EL, Bucala R. Fibrocytes in health and disease. Exp Hematol 2010;38:548–56.
17. Lamouille S, Xu J, Derynck R. Molecular mechanisms of epithelial-mesenchymal transition. Nat Rev Mol Cell Biol 2014; 15:178–96.

18. Humphreys BD, Lin SL, Kobayashi A, Hudson TE, Nowlin BT, Bonventre JV, et al. Fate tracing reveals the pericyte and not epithelial origin on myofibroblasts in kidney fibrosis. Am J Pathol 2010;176:85–97.
19. Kramann R, Schneider RK, DiRocco DP, Machado F, Fleig S, Bondzie PA, et al. Perivascular Gli1+ progenitors are key contributors to injury-induced organ fibrosis. Cell Stem Cell 2015;16:51–66.
20. Zeisberg EM, Taranavski O, Zeisberg M, Dorfman AL, McMullen JR, Gustafsson E, et al. Endothelial-to-mesenchymal transition contributes to cardiac fibrosis. Nat Med 2007;13:952–61.
21. Goumans MJ, van Zonneveld AJ, ten Dijke P. Transforming growth factor β-induced endothelial-to-mesenchymal transition: a switch to cardiac fibrosis? Trends Cardiovasc Med 2008;18: 293–8.
22. Piera-Velazquez S, Li Z, Jimenez SA. Role of endothelial-mesenchymal transition (EndoMT) in the pathogenesis of fibrotic disorders. Am J Pathol 2011;179:1074–84.
23. Piera-Velazquez S, Jimenez SA. Molecular mechanisms of endothelial to mesenchymal cell transition (EndoMT) in experimentally induced fibrotic diseases. Fibrogenesis Tissue Repair 2012;5 Suppl 1:S7.
24. Arciniegas E, Neves CY, Carrillo LM, Zambrano EA, Ramirez R. Endothelial-mesenchymal transition occurs during embryonic pulmonary artery development. Endothelium 2005;12:193–200.
25. Zeisberg EM, Potenta SE, Sugimoto H, Zeisberg M, Kalluri R. Fibroblasts in kidney fibrosis emerge via endothelial-to-mesenchymal transition. J Am Soc Nephrol 2008;19:2282–7.
26. Li J, Qu X, Bertman JF. Endothelial-myofibroblast transition contributes to the early development of diabetic renal interstitial fibrosis in streptozotocin-induced diabetic mice. Am J Pathol 2009;175:1380–8.
27. Hashimoto N, Phan SH, Imaizumi K, Matsuo M, Nakashima H, Kawabe T, et al. Endothelial-mesenchymal transition in bleomycin-induced pulmonary fibrosis. Am J Respir Cell Mol Biol 2010;43: 161–72.
28. LeBleu VS, Taduri G, O'Connell J, Teng Y, Cooke VG, Woda C, et al. Origin and function of myofibroblasts in kidney fibrosis. Nat Med 2012;19:1047–53.
29. Rieder F, Kessler SP, West GA, Bhilocha S, de la Motte C, Sadler TM, et al. Inflammation-induced endothelial-to-mesenchymal transition: a novel mechanism of interstitial fibrosis. Am J Pathol 2011; 179:2660–73.
30. Yoshimatsu Y, Watabe T. Roles of TGF-β signals in endothelial-mesenchymal transition during cardiac fibrosis. Int J Inflam 2011; 724080.
31. Cooley BC, Nevado J, Mellad J, Yang D, St Hilaire C, Negro A, et al. TGF-β signaling mediates endothelial-to-mesenchymal transition (EndMT) during vein graft remodeling. Sci Transl Med 2014;6: 227ra34.
32. Ranchoux B, Antigny F, Rucker-Martin C, Hautefort A, Pechoux C, Bogaard HJ, et al. Endothelial-to-mesenchymal transition in pulmonary hypertension. Circulation 2015;131:1006–18.
33. Good RB, Gilbane AJ, Trinder SL, Denton CP, Coghlan G, Abraham DJ, et al. Endothelial to mesenchymal transition contributes to endothelial dysfunction in pulmonary arterial hypertension. Am J Pathol 2015;185:1850–8.
34. Del Galdo F, Sotgia F, de Almeida CJ, Jasmin JF, Musick M, Lisanti MP, et al. Decreased expression of caveolin 1 in patients with systemic sclerosis: crucial role in the pathogenesis of tissue fibrosis. Arthritis Rheum 2008;58:2854–65.
35. Marelli-Berg FM, Peek E, Lidington EA, Stauss HJ, Lechler RI. Isolation of endothelial cells from murine tissue. J Immunol Methods 2000;244:205–15.
36. Li Z, Jimenez SA. Protein kinase Cδ and c-Abl kinase are required for transforming growth factor β induction of endothelial–mesenchymal transition in vitro. Arthritis Rheum 2011;63: 2473–83.
37. Nolan T, Hands RE, Bustin SA. Quantification of mRNA using real-time RT-PCR. Nat Protoc 2006;1:1559–82.
38. Medici D, Potenta S, Kalluri R. Transforming growth factor-β2 promotes Snail-mediated endothelial mesenchymal transition through convergence of Smad-dependent and Smad-independent signaling. Biochem J 2011;433:515–20.
39. Van Meeteren LA, ten Dijke P. Regulation of endothelial cell plasticity by TGF-β. Cell Tissue Res 2012;347:177–86.
40. Veraldi KL, Hsu E, Feghali-Bostwick CA. Pathogenesis of pulmonary fibrosis in systemic sclerosis: lessons from interstitial lung disease. Curr Rheumatol Rep 2010;12:19–25.
41. Herzog EL, Mathur A, Tager AM, Feghali-Bostwick C, Schneider F, Varga J. Interstitial lung disease associated with systemic sclerosis and idiopathic pulmonary fibrosis: how similar and distinct? [review]. Arthritis Rheumatol 2014;66:1967–78.
42. Wells AU, Margaritopoulos GA, Antoniou KM, Denton C. Interstitial lung disease in systemic sclerosis. Semin Respir Crit Care Med 2014;35:213–21.